

Selective Gas-Phase Cleavage at the Peptide Bond C-Terminal to Aspartic Acid in Fixed-Charge Derivatives of Asp-Containing Peptides

Chungang Gu, George Tsaprailis, Linda Brecci, and Vicki H. Wysocki*

Department of Chemistry, University of Arizona, Tucson, Arizona 85721

This study focuses on the molecular level interpretation of the selective gas-phase cleavage at aspartic acid residues (Asp) in protonated peptides. A $\phi_3\text{P}^+\text{CH}_2\text{C}(=\text{O})^-$ group ($\phi = 2,4,6$ -trimethoxyphenyl) is attached to the N-terminal nitrogen of the selected peptides LDIFSDF and LDIFSDFR, via solid-phase synthesis, to “mimic” the tightly held charge of a protonated arginine (Arg) residue. Collision-induced dissociation in a quadrupole ion trap instrument and surface-induced dissociation in a dual quadrupole instrument were performed for electrospray-generated ions of the fixed-charge peptide derivatives. Selective cleavages at Asp–Xxx are observed for those ions with charge provided only by the fixed charge or for those with a fixed charge and one Arg plus one added proton. This supports a previously proposed mechanism which suggests that the cleavages at Asp–Xxx, initiated by the acidic hydrogen of the Asp residue, become significant when ionizing protons are strongly bound by Arg in the protonated peptides. It is clear that the fixed charge is indeed serving as a “mimic” of protonated Arg and that a protonated Arg side chain is not required to interact with the Asp to induce cleavage at Asp–Xxx. When the number of protons exceeds the number of Arg in a peptide containing Arg and Asp, nonselective cleavages occur. The fragmentation efficiency of the peptides is consistent with the idea that these nonselective cleavages are promoted by a mobile proton. The peptide with a fixed charge and one added proton, $[\phi_3\text{P}^+\text{CH}_2\text{C}(=\text{O})\text{-LDIFSDF} + \text{H}]^{2+}$, fragments much more efficiently than the corresponding peptide with a fixed charge, an Arg and one added proton, $[\phi_3\text{P}^+\text{CH}_2\text{C}(=\text{O})\text{-LDIFSDFR} + \text{H}]^{2+}$; both of these fragment more efficiently than the peptide with a fixed charge and no added proton, $\phi_3\text{P}^+\text{CH}_2\text{C}(=\text{O})\text{-LDIFSDF}$. MS/MS/MS (i.e., MS³) experimental results for b_n ions formed at Asp–Xxx from $\phi_3\text{P}^+\text{CH}_2\text{C}(=\text{O})\text{-LDIFSDF}$ and its H/D exchange derivative, $\phi_3\text{P}^+\text{CH}_2\text{C}(=\text{O})\text{-LDIFSDF-}d_{11}$, are consistent with the b_n ions formed at Asp–Xxx having a succinic anhydride cyclic structure. MS/MS experiments were also carried out for $\phi_3\text{P}^+\text{CH}_2\text{C}(=\text{O})\text{-AAAA}$, a peptide derivative containing active hydrogens only at amide nitrogens plus the C-terminus, and its active H/D exchange product, $\phi_3\text{P}^+\text{CH}_2\text{C}(=\text{O})\text{-AAAA-}d_5$. The results show that a hydrogen originally located at an

amide nitrogen is transferred away in the formation of a cyclic charge remote b ion.

High-throughput peptide sequencing is highly desirable in proteomics and related bioscience. While the conventional method, Edman sequencing, does not fulfill this task, tandem mass spectrometry (MS/MS) provides a means for rapid identification and characterization of peptides/proteins.^{1–4} State-of-the-art mass spectrometry instrumentation and computer technologies have made it possible to run samples in a highly automated fashion. Automated interpretation methods for MS/MS data,^{5–10} e.g., correlation analysis between experimental MS/MS spectra and theoretical MS/MS spectra generated from amino acid sequence stretches in protein or translated DNA databases, have been developed to help solve the bottleneck problem of data interpretation in MS/MS analysis of peptides/proteins. With the foreseeable completion of the Human Genome Project,¹¹ MS/MS studies of peptides/proteins based on correlation analysis using DNA/protein databases could become even more powerful tools in the future. Note that existing algorithms have already taken advantage of the knowledge regarding peptide fragmentation gained by applied and fundamental research performed over the last two decades. However, the current understanding of peptide fragmentation mechanisms is still not sufficient to ensure high correlation between theoretically predicted MS/MS spectra and experimental results. For example, the existing algorithms usually generate a theoretical spectrum such that all the fragment ions within a series occur with the same probability (i.e., the assump-

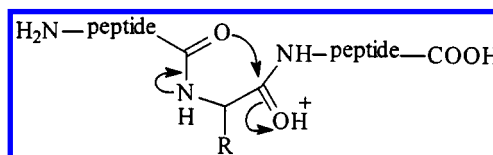
* To whom correspondence should be addressed: (e-mail) vwysoc@u.arizona.edu; (tel) (520)621-2628; (fax) (520)621-8407.

- (1) Roepstorff, P. *Curr. Opin. Biotechnol.* **1997**, *8*, 6–13.
- (2) Shevchenko, A.; Wilm, M.; Mann, M. *J. Protein Chem.* **1997**, *16*, 481–490.
- (3) Dongré, A. R.; Eng, J. K.; Yates, J. R., III *Trends Biotechnol.* **1997**, *15*, 418–425.
- (4) Yates, J., III *J. Mass Spectrom.* **1998**, *33*, 1–19.
- (5) Eng, J. K.; McCormack, A. L.; Yates, J. G., III *J. Am. Soc. Mass Spectrom.* **1994**, *5*, 976–989.
- (6) Yates, J. R., III; Eng, J. K.; McCormack, A. L.; Schieltz, D. *Anal. Chem.* **1995**, *67*, 1426–1436.
- (7) Yates, J. R., III; Eng, J. K.; McCormack, A. L. *Anal. Chem.* **1995**, *67*, 3202–3210.
- (8) Mann, M.; Wilm, M. *Anal. Chem.* **1994**, *66*, 4390–4399.
- (9) Johnson, R. S.; Biemann, K. *Biomed. Environ. Mass Spectrom.* **1989**, *18*, 945–957.
- (10) Hines, W. M.; Falick, A. M.; Burlingame, A. L.; Gibson, B. W. *J. Am. Soc. Mass Spectrom.* **1992**, *3*, 326–336.
- (11) Collins, F.; Patrino, A.; Jordan, E.; Chakravarti, A.; Gesteland, R.; Walters, L. *Science* **1998**, *282*, 682–689.

tion is made that peptide ions cleave nonselectively across the peptide backbone). This is not consistent with experimental observation for selective/enhanced cleavage at certain specific amide linkages. For example, the selective/enhanced cleavages of the amide linkage at the C(O)–N bond C-terminal to an acidic residue (e.g., at Asp–Xxx),^{12–18} or at the C(O)–N bond N-terminal to a proline residue (i.e., Xxx–Pro),^{19,20} have been noticed. However, the fact that these selective/enhanced cleavages do not always occur might have discouraged the investigators from including them in existing computer-based interpretation of peptide MS/MS spectra. Therefore, thorough investigations for improved understanding, on a molecular level, of the enhancement or absence of certain fragment ions in MS/MS experiments are warranted with the long-term goal of providing additional and improved predictive rules for interpretation of peptide MS/MS spectra.

Selective gas-phase cleavage at the peptide bond C-terminal to an Asp residue (i.e., Asp–Xxx) in protonated or sodiated peptide ions has been investigated by several research groups.^{12–17} A succinic anhydride five-membered ring structure has been proposed by Martin and co-workers in this journal,¹² and accepted by other authors,^{16,17,21} as the structure at the “C-terminus” of the N-terminal fragment (either ionic or neutral), following gas-phase cleavage of the Asp–Xxx peptide bond. The involvement of the Asp side-chain carboxylic hydrogen in this fragmentation was confirmed by esterification that blocked the selective/enhanced cleavage at Asp–Xxx.¹² Martin and co-workers proposed a mechanism for cleavage involving proton transfer from the Asp acidic side chain to the adjacent amide nitrogen C-terminal to Asp.¹² To explain the selective cleavage at Asp–Xxx in sodiated peptides, Beauchamp and co-workers suggested a salt bridge model.¹⁶ For singly protonated peptides, Qin and Chait noticed the presence of an arginine residue (Arg) in the peptides that demonstrated selective cleavage at Asp–Xxx.¹⁴ Gaskell and co-workers proposed the involvement of bridging between the Arg and acidic side chains in the enhanced cleavage.^{22,23} MS/MS results for a series of singly protonated oligopeptides X-Leu-Asp-Val-Leu-Gln (X = Arg, Lys, His) showed that the selective cleavage at Asp–Val occurred in the presence of an Arg residue but not when Arg was replaced with other basic amino acid residues (i.e., lysine or histidine).²⁴ This finding is likely related to the fact that arginine

Scheme 1



has the highest gas-phase basicity (GBs) among the 20 common amino acids.^{25–27} Recently, selective cleavage at Asp–Xxx in a series of protonated peptides was investigated by using several different activation methods in a collaboration of the Wysocki group with the groups of Gaskell and Futrell.¹⁷ Selective cleavage at Asp–Xxx was observed only when the number of added protons did not exceed the number of arginines.¹⁷ This suggested that when the ionizing protons are sequestered at arginine, the cleavage catalyzed by the acidic hydrogen of the Asp residue, which requires a seven-membered-ring intermediate, becomes significant.¹⁷ When proton(s) in excess of the number of Arg are available, nonselective cleavage involving the ionizing proton(s) occurs at all backbone residues (e.g., oxazolone formation by nucleophilic attack on a protonated carbonyl^{28–31} via a five-membered ring, see Scheme 1.)

The approach in the present study is to use a fixed-charge chemical group to “mimic” a protonated Arg residue (i.e., an Arg residue that presumably sequesters an ionizing proton). This “mimic” consists of a $\phi_3\text{P}^+-\text{CH}_2\text{C}(=\text{O})$ group ($\phi = 2,4,6$ -trimethoxyphenyl), which is attached to the N-terminal nitrogen of peptides via solid-phase synthesis. As previously reported in this journal by Huang et al. who referred to it as the TMPP–Ac group,³² this fixed-charge group gives virtually no neutral loss from the charged moiety and, thus, does not complicate the interpretation of MS/MS spectra of such peptide derivatives. An immediate goal of the present study is to see whether fixed-charge mimics of Asp-containing peptides previously investigated¹⁷ exhibit fragmentation characteristics similar to those of corresponding protonated peptides with a protonated arginine at the N-terminus.

EXPERIMENTAL SECTION

Synthesis of the N-Terminal Fixed-Charge Derivatives.

Fmoc-Ala-Ala-Ala-Ala, Fmoc-Leu-Asp(OtBu)-Ile-Phe-Ser(tBu)-Asp(OtBu)-Phe, and Fmoc-Leu-Asp(OtBu)-Ile-Phe-Ser(tBu)-Asp(OtBu)-Phe-Arg(Pmc) attached to Wang resin were prepared using solid-phase synthesis protocols outlined by Atherton and Sheppard.³³ The N-terminal Fmoc (9-fluorenylmethoxycarbonyl) protecting

(12) Yu, W.; Vath, J. E.; Huberty, M. C.; Martin, S. A. *Anal. Chem.* **1993**, *65*, 3015–3023.

(13) Bakhtiar, R.; Wu, Q.; Hofstadler, S. A.; Smith, R. D. *Biol. Mass Spectrom.* **1994**, *23*, 707–710.

(14) Qin, J.; Chait, B. T. *J. Am. Chem. Soc.* **1995**, *117*, 5411–5412.

(15) Jockusch, R. A.; Schnier, P. D.; Price, W. D.; Strittmatter, E. F.; Demirev, P. A.; Williams, E. R. *Anal. Chem.* **1997**, *69*, 1119–1126.

(16) Lee, S.; Hyun, S. K.; Beauchamp, J. L. *J. Am. Chem. Soc.* **1998**, *120*, 3188–3195.

(17) Tsapraillis, G.; Nair, H.; Somogyi, Á.; Wysocki, V. H.; Zhong, W.; Futrell, J. H.; Summerfield, S. G.; Gaskell, S. J. *J. Am. Chem. Soc.* **1999**, *121*, 5142–5154.

(18) Tsapraillis, G.; Somogyi, Á.; Nikolaev, E. N.; Wysocki, V. H. *Int. J. Mass Spectrom.* **2000**, *195/196*, 467–479.

(19) Loo, J. A.; Edmonds, C. G.; Smith, R. D. *Anal. Chem.* **1993**, *65*, 425–438.

(20) Vaisar, T.; Urban, J. *J. Mass Spectrom.* **1996**, *31*, 1185–1187.

(21) Liao, P.-C.; Huang, Z.-H.; Allison, J. *J. Am. Soc. Mass Spectrom.* **1997**, *8*, 501–509.

(22) Cox, K. A.; Gaskell, S. J.; Morris, M.; Whiting, A. *J. Am. Soc. Mass Spectrom.* **1996**, *7*, 522–531.

(23) Burlet, O.; Yang, C. Y.; Gaskell, S. J. *J. Am. Soc. Mass Spectrom.* **1992**, *3*, 337–344.

(24) Gu, C.; Somogyi, Á.; Wysocki, V. H.; Medzihradzsky, K. F. *Anal. Chim. Acta* **1999**, *397*, 247–256.

(25) Wu, Z.; Fenselau, C. *Rapid Commun. Mass Spectrom.* **1992**, *6*, 403–405.

(26) Gorman, G. S.; Speir, J. P.; Turner, C. A.; Amster, I. J. *J. Am. Chem. Soc.* **1992**, *114*, 3986–3988.

(27) Hunter, E. P. L.; Lias, S. G. *J. Phys. Chem. Ref. Data* **1998**, *27*, 413–656 (data cited also available at <http://webbook.nist.gov/chemistry/>).

(28) Arnott, D.; Kottmeier, D.; Yates, N.; Shabanowitz, J.; Hunt, D. F. *The 42nd ASMS Conference on Mass Spectrometry*, Chicago, IL, 1994; p 470.

(29) Summerfield, S. G.; Bolgar, M. S.; Gaskell, S. J. *J. Mass Spectrom.* **1997**, *32*, 225–231.

(30) Yalcin, T.; Khouw, C.; Csizmadia, I. G.; Peterson, M. R.; Harrison, A. G. *J. Am. Soc. Mass Spectrom.* **1995**, *6*, 1164–1174.

(31) Yalcin, T.; Csizmadia, I. G.; Peterson, M. R.; Harrison, A. G. *J. Am. Soc. Mass Spectrom.* **1996**, *7*, 233–242.

(32) Huang, Z. H.; Wu, J.; Roth, K. D. W.; Yang, Y.; Gage, D. A.; Watson, J. T. *Anal. Chem.* **1997**, *69*, 137–144.

group of the peptides was removed by piperidine in *N,N*-dimethylformamide (DMF). The resin-bound peptides (0.037 mmol) with the free N-terminus (active side chains still protected) were then reacted with 0.10 mmol of iodoacetic anhydride in anhydrous DMF for 25 min, washed by DMF twice, and reacted with 0.15 mmol of tris(2,4,6-trimethoxyphenyl)phosphine in toluene/DMF (1:1; v/v) for 90 min. Following this, the resin-bound fixed-charge derivatives were washed with toluene, DMF, and then dichloromethane. Finally, the peptide derivatives, tris(2,4,6-trimethoxyphenyl)phosphonium-acetyl-Leu-Asp-Ile-Phe-Ser-Asp-Phe, and tris(2,4,6-trimethoxyphenyl)phosphonium-acetyl-Leu-Asp-Ile-Phe-Ser-Asp-Phe-Arg were cleaved from the resin and any protected amino acid side chains were deprotected using a 1.5-mL mixture of trifluoroacetic acid (TFA)/H₂O/1,2-ethanedithiol (95:2.5:2.5; v/v/v). Tris(2,4,6-trimethoxyphenyl)phosphonium-acetyl-Ala-Ala-Ala was cleaved from the resin with TFA/H₂O (95:5; v/v). The Fmoc derivatives of the amino acids required for the synthesis were obtained from Novabiochem or Advanced Chemtech. The C-terminal residue for the synthesis was purchased already attached to Wang resin from Novabiochem or Advanced Chemtech. Once a peptide derivative was precipitated in diethyl ether, its identity and purity were confirmed by electrospray ionization mass spectrometry. Hereafter, the peptide derivatives are referred to as $\phi_3\text{P}^+\text{CH}_2\text{C}(=\text{O})\text{-LDIFSDF}$, $\phi_3\text{P}^+\text{CH}_2\text{C}(=\text{O})\text{-LDIFSDFR}$, and $\phi_3\text{P}^+\text{CH}_2\text{C}(=\text{O})\text{-AAAA}$ ($\phi = 2,4,6\text{-trimethoxyphenyl}$).

Electrospray Ionization (ESI)/Collision-Induced Dissociation (CID) In an Ion Trap. Low-energy CID experiments, which involve collision of mass-selected ions into a target gas, were carried out on a Finnigan quadrupole ion trap mass spectrometer (LCQ). The precipitated fixed-charge peptide derivatives were dissolved in a solution of MeOH/H₂O (70:30; v/v) containing 0.2% acetic acid to give a concentration of 20–100 pmol/ μL . The peptide derivative solutions were then injected into the ESI source at a flow rate of 3 $\mu\text{L}/\text{min}$. The applied voltage on the needle of the ESI source was 4.8 kV and the capillary temperature was maintained at 200 °C for all samples. Unit mass selection of the precursor ion was performed. The operational parameter that controls the excitation energy in MS/MS or MS/MS/MS (i.e., MS³) mode (indicated as “% relative collision energy” by the manufacturer) was incremented in small steps to monitor low-energy fragmentation processes for the precursor ions selected. The collision gas was helium. In the ion trap, energy is deposited in approximately a thermal distribution. Because of the stepwise, multistep nature of the energy deposition, lower energy processes are often favored over higher energy processes.^{34,35}

CID experiments were also performed in the ion trap instrument for active hydrogen/deuterium (H/D) exchange derivatives of $\phi_3\text{P}^+\text{CH}_2\text{C}(=\text{O})\text{-LDIFSDF}$ and $\phi_3\text{P}^+\text{CH}_2\text{C}(=\text{O})\text{-AAAA}$. The fixed-charge derivative $\phi_3\text{P}^+\text{CH}_2\text{C}(=\text{O})\text{-LDIFSDF}$ or $\phi_3\text{P}^+\text{CH}_2\text{C}(=\text{O})\text{-AAAA}$ was first dissolved in deuterated CH₃OD solvent containing 0.5% CD₃COOD for ~20 min, after which it was introduced into the ESI source via infusion. The infusion line was precleaned with CH₃OD. Finally, the CID spectra of $\phi_3\text{P}^+\text{CH}_2\text{C}(=\text{O})\text{-LDIFSDF-}d_{11}$ or $\phi_3\text{P}^+\text{CH}_2\text{C}(=\text{O})\text{-AAAA-}d_5$ were acquired.

(33) Atherton, E.; Sheppard, R. C. In *Solid-Phase Peptide Synthesis: A Practical Approach*; Rickwood, D., Hames, B. D., Eds.; Oxford University Press: Oxford, U.K., 1989.

(34) Goeringer, D. E.; Asano, K. G.; McLuckey, S. A. *Int. J. Mass Spectrom.* **1999**, *183*, 275–288.

Electrospray Ionization/Surface-Induced Dissociation (SID)

SID involves collisions of mass-selected ions with a target surface. The instrument used for SID experiments is a dual quadrupole tandem mass spectrometer specifically designed for low-energy ion surface collisions and has been described previously.^{17,36–38} It is composed of two Extrel 4000 u quadrupoles positioned at 90° with the target surface placed between the two quadrupoles. Incident angles of the precursor ion beam are 45°–50° with respect to the surface normal. The ESI source used in the SID instrument is a heated capillary design based on those of Chowdhury et al.³⁹ and Papac et al.⁴⁰ The solutions (same as those described in the CID experiments) were sprayed at atmospheric pressure from a syringe needle held at 4.0–4.8 kV (flow rate of 2 $\mu\text{L}/\text{min}$), toward a metal capillary (120 V) maintained at 130 °C. The ions were directed toward a skimmer cone (90 V) and entered into the high-vacuum region of the mass spectrometer. The SID collision energy is defined by the voltage difference between the skimmer and the collision surface multiplied by the charge state of the ions. The collision target surface used in the SID experiments was a self-assembled monolayer (SAM) of 2-(perfluorodecyl)ethanethiol on gold (i.e., CF₃(CF₂)₉CH₂CH₂SAu) prepared by procedures described previously.^{17,41} With this surface, the average conversion of kinetic energy to internal energy has been estimated to be 20–30%.^{42–44} In addition to different energy deposition functions corresponding to SID and ion trap CID, these experiments also have different time frames for dissociation with only microseconds allowed for dissociation in the Q-surface-Q instrument and milliseconds to seconds in the ion trap.

SID mass spectra were obtained over a range of collision energies. SID fragmentation efficiencies, defined as the ratio of

$$\frac{\sum(\text{fragment ion peak areas})}{(\text{parent ion peak area}) + \sum(\text{fragment ion peak areas})}$$

were plotted as a function of collision energy (eV) for ESI-generated ions of the Asp-containing fixed-charge peptide derivatives. The curve fittings for the raw data points were performed using the function

$$f(x) = \frac{a - d}{1 + (x/c)^b} + d \quad (1)$$

where *a*, *b*, *c*, and *d* are the fitting parameters. The final value of

(35) McLuckey, S. A.; Goeringer, D. E. *J. Mass Spectrom.* **1997**, *32*, 461–474.

(36) Wysocki, V. H.; Ding, J.-M.; Jones, J. L.; Callahan, J. H.; King, F. L. *J. Am. Soc. Mass Spectrom.* **1992**, *3*, 27–32.

(37) Dongré, A. R.; Somogyi, Á.; Wysocki, V. H. *J. Mass Spectrom.* **1996**, *31*, 339–350.

(38) McCormack, A. L.; Somogyi, Á.; Dongré, A. R.; Wysocki, V. H. *Anal. Chem.* **1993**, *65*, 2859–2872.

(39) Chowdhury, S. K.; Katta, V.; Chait, B. T. *Rapid Commun. Mass Spectrom.* **1990**, *4*, 81–87.

(40) Papac, D. I.; Schey, K. L.; Knapp, D. R. *Anal. Chem.* **1991**, *63*, 1658–1660.

(41) Dongré, A. R.; Jones, J. L.; Somogyi, Á.; Wysocki, V. H. *J. Am. Chem. Soc.* **1996**, *118*, 8365–8374.

(42) Miller, S. A.; Riederer, D. E., Jr.; Cooks, R. G.; Cho, W. R.; HW, L.; H, K. J. *Phys. Chem.* **1994**, *98*, 245–251.

(43) Morris, M.; Riederer, D. E., Jr.; Cooks, R. G.; Ast, T.; Chidsey, C. E. D. *Int. J. Mass Spectrom. Ion Processes* **1992**, *122*, 181–217.

(44) Vékey, K.; Somogyi, Á.; Wysocki, V. H. *J. Mass Spectrom.* **1995**, *30*, 212–217.

c corresponds to the value of *x* at the inflection point of the SID efficiency curve. The ESI/SID fragmentation efficiency curves provide a measure of relative fragmentation energetics of the selected ions.

RESULTS AND DISCUSSION

MS/MS Spectra of the Asp-Containing Fixed-Charge Derivatives. Two different methods, low-energy CID in an ion-trap instrument and SID in a quadrupole tandem mass spectrometer, were utilized to obtain the spectra discussed below. These methods were chosen because they deposit different distributions of internal energy and allow different time frames for dissociation. In previous work on peptides containing a protonated arginine and acidic residues, we have shown selective cleavages at acidic residues to persist throughout a range of instrument types and dissociation time frames.^{17,18,24} Labeling of peaks in the spectra follows the nomenclature defined by Roepstorff and Fohlman⁴⁵ and modified by Biemann.^{46,47} For example, *b_n* or *y_n* designates the N-terminal or the C-terminal charged fragment, respectively, where cleavage occurs at the *n*th peptide bond (counting from the N- or C-terminus, respectively). The ions that formally correspond to a loss of 28 amu (CO) from *b_n* ions are called *a_n* ions.

(A) Electrospray Ionization/Low-Energy Collision-Induced Dissociation in the Ion Trap Instrument. Figure 1 shows ESI/low-energy CID spectra obtained with the ion trap instrument for derivatized peptides in which the $\phi_3\text{P}^+\text{CH}_2\text{C}(=\text{O})$ group is attached to the N-terminus of the Asp-containing peptides, LDIFSDF and LDIFSDFR. The singly charged $\phi_3\text{P}^+\text{CH}_2\text{C}(=\text{O})$ -LDIFSDF ions cleave selectively at the DI and DF peptide bonds to give b-type N-terminal fragment ions (*b₂* and *b₆* ions, respectively; Figure 1a). The peak at *m/z* 573 corresponds to the fixed-charge group (i.e., fragment $\phi_3\text{P}^+\text{CH}=\text{C}=\text{O}$).³² Note that at relatively higher collision energies when other fragment ions occur or even when the precursor ion peak disappears, *b₂* and *b₆* ions are still the dominant fragment ions among other fragment ions, including *d₂* ions, *d₆* ions, and *b_n*/*a_n* ion pairs at positions other than Asp residue positions (spectrum available in Supporting Information). When an ionizing proton is added to $\phi_3\text{P}^+\text{CH}_2\text{C}(=\text{O})$ -LDIFSDF to form an $[\text{M} + \text{H}]^{2+}$ ion, the dissociation pattern changes dramatically. The doubly charged $[\text{M} + \text{H}]^{2+}$ ions of the derivative $\phi_3\text{P}^+\text{CH}_2\text{C}(=\text{O})$ -LDIFSDF, with one charge provided by the phosphonium group and the other by an ionizing proton, cleave nonselectively along the whole peptide backbone as demonstrated by the presence of the entire *b_n* ion series (Figure 1b). However, when an Arg and one added proton are present in the peptide $\phi_3\text{P}^+\text{CH}_2\text{C}(=\text{O})$ -LDIFSDFR, the doubly charged $[\text{M} + \text{H}]^{2+}$ ions cleave selectively at two Asp–Xxx peptide bonds (Figure 1c). Complementary *b₆*/*y₂* and *b₂*/*y₆* ion pairs produced by cleavage of the DF and DI peptide bonds, respectively, dominate the spectrum (Figure 1c). The lower intensity of the *y₂* ion, relative to that of the *b₆* ion in the *b₆*/*y₂* complementary pair, is the result of the mass discrimination that occurs near the low-mass cutoff end of ion trap MS/MS mode.^{48,49} It is noteworthy that, on the dissociation of the singly charged $\phi_3\text{P}^+\text{CH}_2\text{C}(=\text{O})$ -

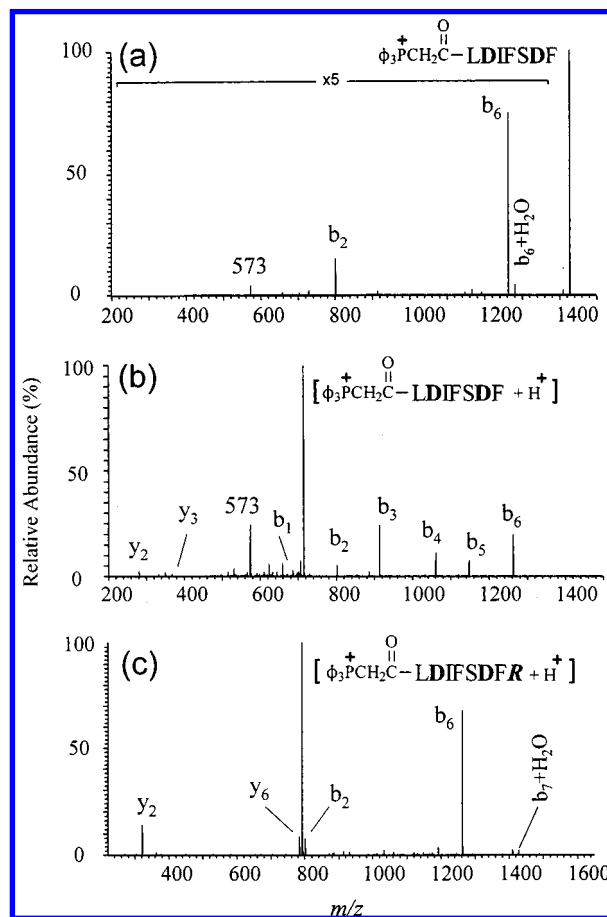


Figure 1. ESI/low-energy CID spectra of (a) M^+ ions of $\phi_3\text{P}^+\text{CH}_2\text{C}(=\text{O})$ -LDIFSDF, (b) $[\text{M} + \text{H}]^{2+}$ ions of $\phi_3\text{P}^+\text{CH}_2\text{C}(=\text{O})$ -LDIFSDF, and (c) $[\text{M} + \text{H}]^{2+}$ ions of $\phi_3\text{P}^+\text{CH}_2\text{C}(=\text{O})$ -LDIFSDFR; obtained in a Finnigan ion trap mass spectrometer (LCQ) using helium as collision gas. The “% relative collision energy” (defined by the instrument manufacturer) used for acquiring the spectra in parts a–c was 38.5, 24.3, and 20.7%, respectively.

LDIFSDFR ions, dominant *b₂* and *b₆* ions are also observed along with an abundant H_2O loss peak and an abundant *b₇* + H_2O ion (spectrum available in Supporting Information; formation of *b₇* + H_2O discussed below).

(B) Electrospray Ionization/Surface-Induced Dissociation in the Tandem Quadrupole Instrument. Figure 2 shows the ESI/SID spectra for the same parent ions as those shown in Figure 1. SID spectra often differ in appearance from those presented for low-energy CID in the ion trap (Figure 2 vs 1) due to different distributions of internal energy and different time frames for dissociation. However, inherent similarities can be readily seen. For example, the complementary *b₆*/*y₂* ion pair dominates in the MS/MS spectra of $[\phi_3\text{P}^+\text{CH}_2\text{C}(=\text{O})\text{-LDIFSDFR} + \text{H}^+]^{2+}$ (Figures 2c and 1c), while nonselective cleavages occur at all the peptide bonds for the $[\text{M} + \text{H}]^{2+}$ ions of $\phi_3\text{P}^+\text{CH}_2\text{C}(=\text{O})$ -LDIFSDF (e.g. an entire series of *b_n* ions as well as some y-type ions are observed; Figures 2b and 1b). Much higher intensity ratios of *a_n*/*b_n* ions are observed for doubly charged $[\text{M} + \text{H}]^{2+}$ ions of $\phi_3\text{P}^+\text{CH}_2\text{C}(=\text{O})$ -LDIFSDF by SID (Figure 2b) than by low-

(45) Roepstorff, P.; Fohlman, J. *Biomed. Mass Spectrom.* **1984**, *11*, 601–603.

(46) Johnson, R. S.; Martin, S. A.; Biemann, K. *Int. J. Mass Spectrom. Ion Processes* **1988**, *86*, 137–154.

(47) Biemann, K. *Methods Enzymol.* **1990**, *193*, 455–479.

(48) Louris, J. N.; Cooks, R. G.; Syka, J. E. P.; Kelley, P. E.; Stafford, G. C.; Todd, J. F. *J. Anal. Chem.* **1987**, *59*, 1677–1685.

(49) Paradisi, C.; Todd, J. F. J.; Traldi, P.; Vettori, U. *Org. Mass Spectrom.* **1992**, *27*, 251–254.

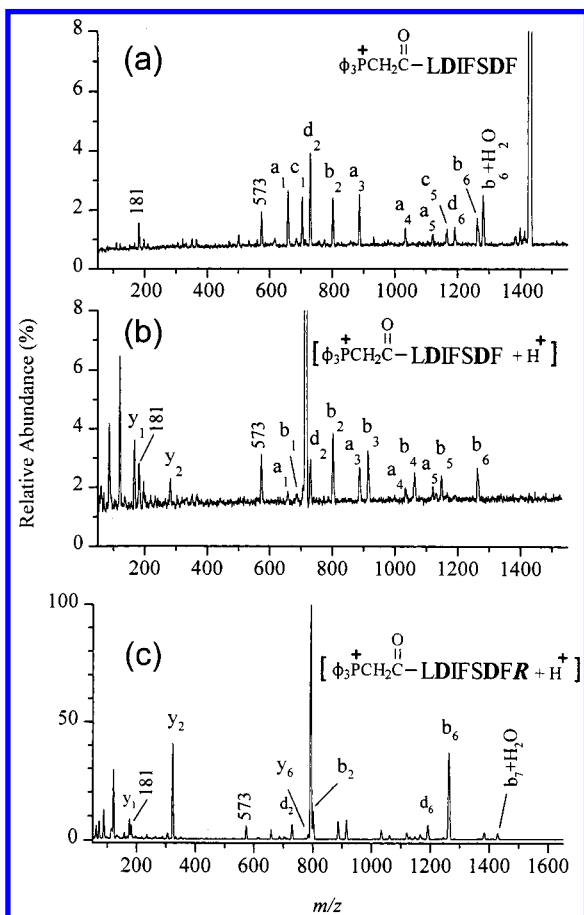


Figure 2. ESI/SID spectra of (a) M^+ ions of $\phi_3P^+CH_2C(=O)$ -LDIFSDF at a collision energy of 65 eV, (b) $[M + H]^{2+}$ ions of $\phi_3P^+CH_2C(=O)$ -LDIFSDF at a collision energy of 15 eV, and (c) $[M + H]^{2+}$ ions of $\phi_3P^+CH_2C(=O)$ -LDIFSDFR at a collision energy of 65 eV. In all cases, a SAM of 2-(perfluorodecyl)ethanethiol on gold (i.e., $CF_3(CF_2)_9CH_2CH_2S-Au$) was used as the collision target surface. Note that the peptide precursor ion peaks in (a) and (b) are off scale.

energy CID in the ion trap (Figure 1b, a_n -type ions not labeled due to very low intensities). The peak at m/z 181 corresponds to the fragment ϕCH_2^+ ($\phi = 2,4,6$ -trimethoxyphenyl) that has been suggested as a further dissociation product via a skeletal rearrangement³² of the fragment ion at m/z 573 ($\phi_3P^+CH=C=O$).

In the SID spectrum of singly charged $\phi_3P^+CH_2C(=O)$ -LDIFSDF ions (Figure 2a), the only b-type ions present are those corresponding to the cleavage at the two C(=O)-N positions C-terminal to the Asp residues (b_2 and b_6); a_n series ions occur at other positions. In addition, d_2 and c_1 ions, as well as d_6 and c_5 ions, corresponding to cleavage adjacent to the two Asp residues are observed (Figure 2a). It is of interest that the SID results shown in Figure 2a are similar to those obtained previously with MALDI/PSD or FAB/keV CID for the N-terminal fixed-charge derivatives of other Asp-containing peptides.^{21,50} In all of these experiments,^{21,50} as well as in ion trap CID at relatively higher collision energies for singly charged ions of fixed-charge peptide derivatives (spectrum available in Supporting Information), occurrences of b_n , d_n , and c_{n-1} ions at the Asp residue of the n th

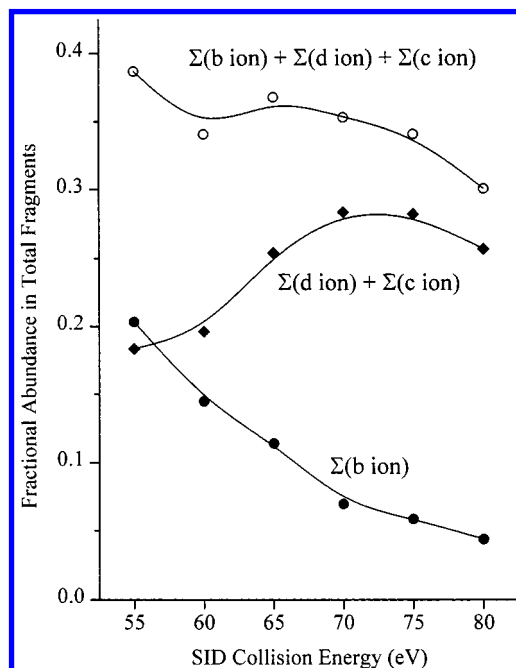


Figure 3. The abundance of b_n , d_n , and c_{n-1} ($n = 2, 6$) versus total abundance of all fragment ions, i.e., fractional abundance, as a function of SID collision energy, recorded when $\phi_3P^+CH_2C(=O)$ -LDIFSDF singly charged ions collide with a SAM surface of $CF_3(CF_2)_9CH_2CH_2S-Au$. The fractional abundance has been summed up in such a way as to clearly indicate the trends discussed in the text.

position, in addition to a-type ions at all other residues, are observed. Watson and co-workers recently suggested that the occurrence of b_n , d_n , and c_{n-1} ions be used to identify an Asp in peptide sequences of $\phi_3P^+-CH_2C(=O)$ -derivatized tryptic digests of proteins.⁵¹ Gaskell and co-workers previously noted d_n and c_{n-1} ion formation from b_n ions produced by Asp-Xxx cleavage.⁵² Furthermore, occurrences of d_n and c_{n-1} , along with b_n , at the Asp residue of the n th position, have also been observed for singly protonated peptides containing an Arg (presumably protonated Arg) at the N-termini.^{18,24}

Formation of d_n/c_{n-1} at the Asp Residue of the n th Position. Different approaches described below were used to investigate whether the d_n/c_{n-1} at the Asp residue of the n th positions (Figure 2a) can be produced from the corresponding b_n ion. First, as shown in Figure 3, the fractional abundance of the ions related to the two Asp residues is plotted as a function of SID collision energy. From this figure it is seen that, as the collision energy increases, the fractional abundance of $[\Sigma(d \text{ ion}) + \Sigma(c \text{ ion})]$ increases whereas that of the $\Sigma(b \text{ ion})$ decreases. This dependence of abundance ratio of $(\Sigma d + \Sigma c)/\Sigma b$ on the collision energy suggests that the d_2/c_1 and d_6/c_5 ions corresponding to cleavage at the Asp positions (Figure 2a) are produced from the b_2 and b_6 ions, respectively. This was further investigated as described below.

MS/MS/MS (i.e., MS^3) experiments were performed in the ion trap instrument. As shown in Figure 4a, after generation of the b_2 ion from $\phi_3P^+CH_2C(=O)$ -LDIFSDF under MS/MS CID

(50) Spengler, B.; Luetzenkirchen, F.; Metzger, S.; Chauand, P.; Kaufmann, R.; Jeffery, W.; Barlet-Jones, M.; Pappin, D. J. C. *Int. J. Mass Spectrom. Ion Processes* **1997**, *169*, 127–140.

(51) Sadagopan, N.; Watson, J. T. *J. Am. Soc. Mass Spectrom.* **2000**, *11*, 107–119.

(52) Summerfield, S. G.; Whiting, A.; Gaskell, S. J. *Int. J. Mass Spectrom. Ion Process* **1997**, *162*, 149–161.

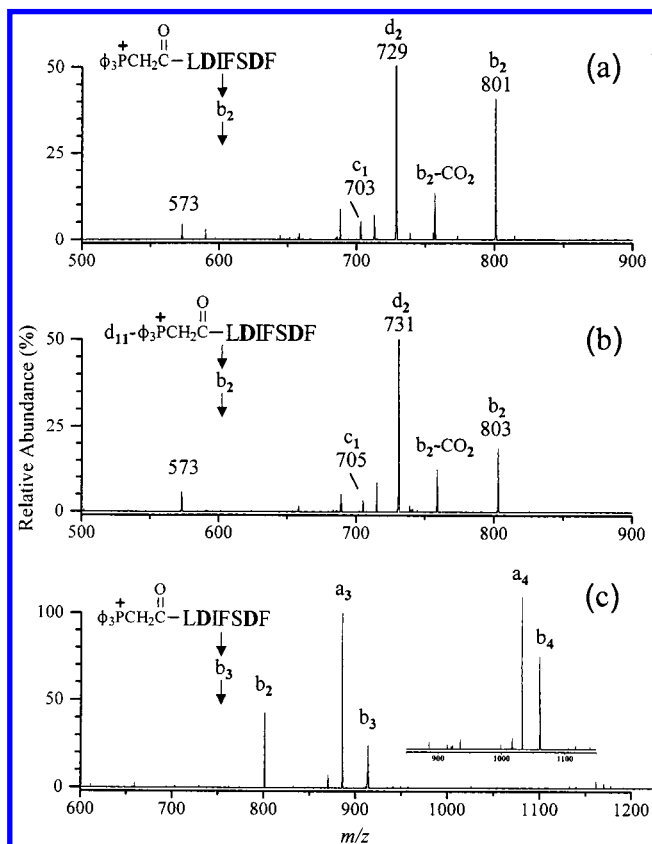


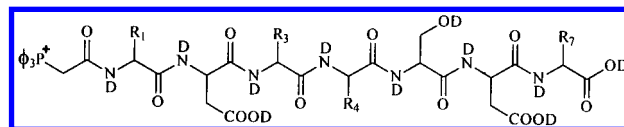
Figure 4. Following MS/MS CID in the ion trap instrument, the MS/MS (i.e., MS³) CID spectra acquired for (a) b₂ ions (*m/z* 801) produced from $\phi_3\text{P}^+\text{CH}_2\text{C}(=\text{O})\text{-LDIFSDF}$, (b) b₂ ions (*m/z* 803, containing two deuterium atoms) produced from the H/D exchanged derivative $\phi_3\text{P}^+\text{CH}_2\text{C}(=\text{O})\text{-LDIFSDF-d}_{11}$; and (c) b₃ ions and b₄ ions (inset) produced from $\phi_3\text{P}^+\text{CH}_2\text{C}(=\text{O})\text{-LDIFSDF}$.

conditions, the b₂ ion (*m/z* 801) was selected and subjected to MS³ using CID. It is seen in Figure 4a that d₂ and c₁ ions can be produced from b₂ ions. It is worth noting that dissociation of the d₂ ions of $\phi_3\text{P}^+\text{CH}_2\text{C}(=\text{O})\text{-LDIFSDF}$ gives *no* trace of c₁ ions (MS³ spectrum available in Supporting Information); i.e., both d₂ and c₁ are products of b₂ fragmentation. Additionally, dissociation of the b₆ ions of $\phi_3\text{P}^+\text{CH}_2\text{C}(=\text{O})\text{-LDIFSDF}$ gives d₆, c₅, b₂, d₂, and c₁ ions (MS³ spectrum available in Supporting Information).

Finally, $\phi_3\text{P}^+\text{CH}_2\text{C}(=\text{O})\text{-LDIFSDF-d}_{11}$, produced by H/D exchange (see Experimental Section) and consistent with deuterium at each of the C(O)NH active sites as well as each of the carboxylic acid and serine OH groups, was fragmented under MS/MS CID conditions in the ion trap (spectrum available in Supporting Information). The masses recorded for b_{*n*}, d_{*n*}, and c_{*n-1*} fragment ions at Asp residues of labeled and unlabeled precursor ions are listed in Table 1. Following the MS/MS fragmentation, the b₂ ion (*m/z* 803) containing two deuterium atoms was selected and a MS³ spectrum was acquired and is provided in Figure 4b. Note that both c₁ and d₂ ions contain two deuterium atoms (MS³ spectrum in Figure 4b, as well as MS/MS data in Table 1).

Plausible pathways for dissociation of the b_{*n*} ions produced by Asp–Xxx cleavage are proposed in Scheme 2. The d_{*n*} ion occurring at the Asp residue of the *n*th position can be formed by loss of a CO₂ and a CO molecule from the five-membered-ring anhydride structure (Scheme 2a). Note that this is different from a previously reported mechanism for *common* d_{*n*} ion formation in

Table 1. Ion Mass-to-Charge Values of M⁺, b, d, and c Ions Produced by MS/MS of Unlabeled and Labeled $\phi_3\text{P}^+\text{CH}_2\text{C}(=\text{O})\text{-LDIFSDF}$

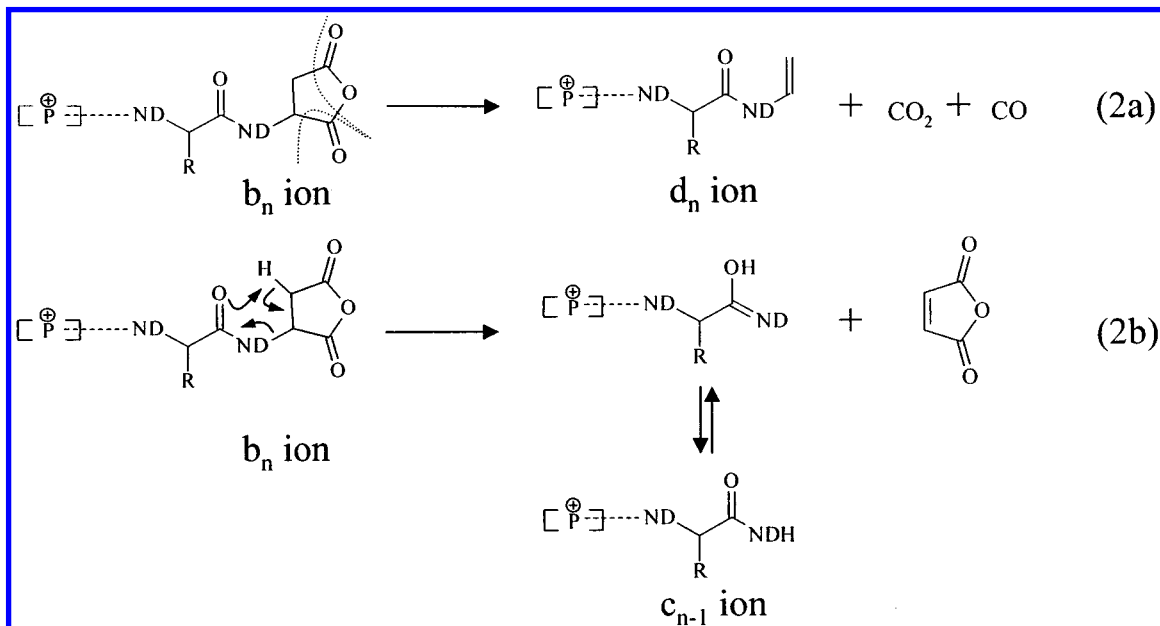


	observed mass		no. of D's
	unlabeled	labeled	
M ⁺	1428.4	1439.5	+11
b ₆	1263.3	1271.3	+8
d ₆	1191.4	1199.4	+8
c ₅	1165.6	1173.2	+8
b ₂	801.1	803.2	+2
d ₂	729.3	731.3	+2
c ₁	703.3	705.1	+2

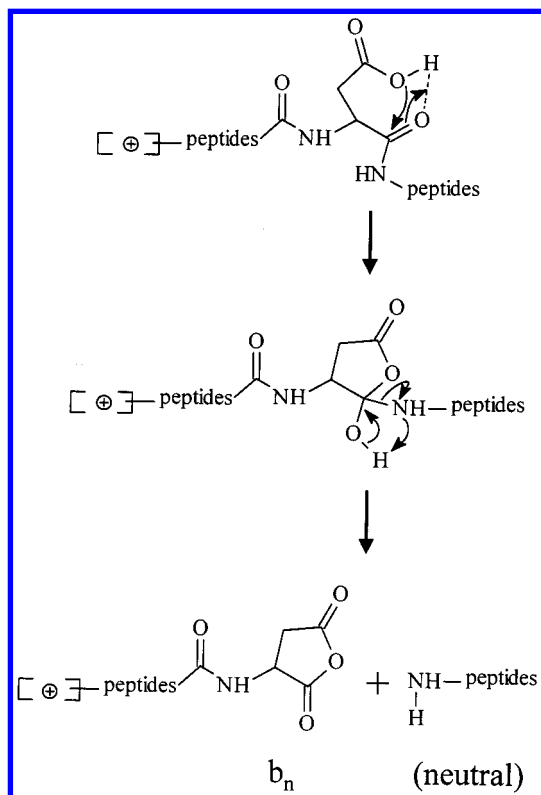
which a common d_{*n*} ion forms via an (a_{*n*}+1) radical ion.⁴⁶ Migration of a hydrogen from the anhydride structure to the adjacent carbonyl oxygen N-terminal to the Asp residue, via a six-membered ring, can lead to formation of a tautomer of the c_{*n-1*} ion, with concomitant loss of a neutral molecule of maleic anhydride (Scheme 2b). The numbers of deuterium atoms in b₂ and b₆ ions alone (Table 1) are not direct evidence for, but are consistent with, the cyclic anhydride structure of these b ions. As illustrated with Scheme 2, the MS/MS data (Table 1) and MS³ results (Figure 4a,b) obtained for labeled and unlabeled $\phi_3\text{P}^+\text{CH}_2\text{C}(=\text{O})\text{-LDIFSDF}$ are consistent with the previously proposed anhydride formation for the b_{*n*} ions formed at Asp–Xxx.^{12,16,17,21} Further fragmentation of these anhydride b_{*n*} ions produces d_{*n*} and c_{*n-1*} ions, which contain the same number of deuterium atoms as the b_{*n*} ion, consistent with Scheme 2. In contrast to these ions formed at Asp–Xxx, it is shown in Figure 4c that the b_{*n*} ions produced at positions other than C-terminal to Asp do not lose CO and CO₂, but rather fragment by loss of CO to form a_{*n*} ions. The production of b₂ from b₃, in addition to a₃, on MS³ of the b₃ from $\phi_3\text{P}^+\text{CH}_2\text{C}(=\text{O})\text{-LDIFSDF}$, is rationalized below in the section on the structure of generic charge-remote b ions.

Mechanism for Selective Cleavage at Asp–Xxx. We show a mechanism in Scheme 3 for the formation of b_{*n*} ions at Asp–Xxx linkages in the presence of a fixed charge. The “remote” positive charge in this scheme represents the quaternary phosphonium in the fixed-charge peptide derivatives or a protonated Arg residue in protonated Arg-containing peptides as previously reported.¹⁷ H-bonding to the amide oxygen promotes the nucleophilic attack of the Asp side-chain carboxyl oxygen on the amide carbonyl carbon by making the carbonyl *carbon* of the Asp–Xxx amide bond electropositive (Scheme 3). The H-bonded intermediate that promotes nucleophilic attack was found in molecular modeling calculations previously reported.¹⁸ In that work, out of ~10 000 gas-phase conformers of singly protonated RGDGGGDG sampled, ~5% were found to have favorable H-bonds between the acidic hydrogen of either the third and/or seventh aspartic acid and their adjacent amide oxygen.¹⁸ Subsequently (as shown in Scheme 3), the five-membered-ring intermediate is formed, and upon a hydrogen rearrangement and cleavage of the C–N bond, the b_{*n*} ion with a substituted succinic anhydride cyclic structure

Scheme 2



Scheme 3



is produced. It should be noted that if the "remote" positive charge (e.g., a protonated Arg) were to be located somewhere on the C-terminal side of the Asp residue, the succinic anhydride would be the terminating structure of a *neutral* N-terminal fragment and consequently, an *ionic* C-terminal fragment (i.e., a y-type ion) would occur upon the cleavage of Asp–Xxx (refer to the MS/MS spectra in refs 12, 14, and 17).

MS/MS/MS of the b_6 ion from $[\phi_3\text{P}^+\text{CH}_2\text{C}(=\text{O})\text{-LDIFSDF} + \text{H}]^{2+}$ produced a spectrum (available in Supporting Information) similar to that in Figure 4a and b (loss of CO_2 and CO), suggesting

that the anhydride product ion structure is produced at Asp–Xxx even in the presence of an ionizing proton. To explain this product, Scheme 3 needs to be modified only slightly: an ionizing proton present at the carbonyl oxygen being attacked by the carboxylic OH of Asp simplifies the mechanism shown in Scheme 3 by not requiring the initial seven-membered-ring formation. By contrast, MS^3 of the b_4 ion of $[\phi_3\text{P}^+\text{CH}_2\text{C}(=\text{O})\text{-LDIFSDF} + \text{H}]^{2+}$ produces mainly the a_4 ion. For peptides with an Arg and one ionizing proton (a sequestered charge) but no fixed charge, the MS^3 results parallel those for the fixed-charge derivatives; i.e., cleavage at Asp and further fragmentation of the corresponding b_n ion leads to d_n and c_{n-1} ions while cleavage at a residue such as Phe and further fragmentation of the corresponding b_n ion leads to the a_n ion. The above cases of Asp–Xxx cleavage correspond to a final product in which charge is present at the amino terminus and the new carboxy terminus of the amino terminal fragment is the neutral anhydride. When there is no fixed charge and no Arg, e.g., when $[\text{LDIFSDF} + \text{H}]^+$ is fragmented, further fragmentation of the b_6 ion (the ion produced by cleavage of the DF bond) is dominated by H_2O loss and not formation of d_6 and c_5 while further fragmentation of the b_4 ion (the ion produced by cleavage of the FS bond) leads to the a_4 ion (spectra available in Supporting Information). In this case, where there is no fixed charge and no sequestration of the ionizing charge (no Arg), there is no distinctive "signature" for cleavage at Asp and it is not clear whether the product ion structure is a protonated anhydride or some other structure.

The Structure of "Generic" Charge Remote b_n Ions Generated from Peptides Derivatized To Contain a Fixed Charge and No Ionizing Proton. In the sections above, strong experimental evidence is provided that supports an anhydride structure for b ions produced by Asp–Xxx cleavage. In peptides with a fixed charge, the anhydride structure of the Asp b ions is supported in two cases: with no added charge (charge-remote b ion formation) and also in the case where a proton is added to a peptide that has a fixed charge (charge-directed b ion formation).

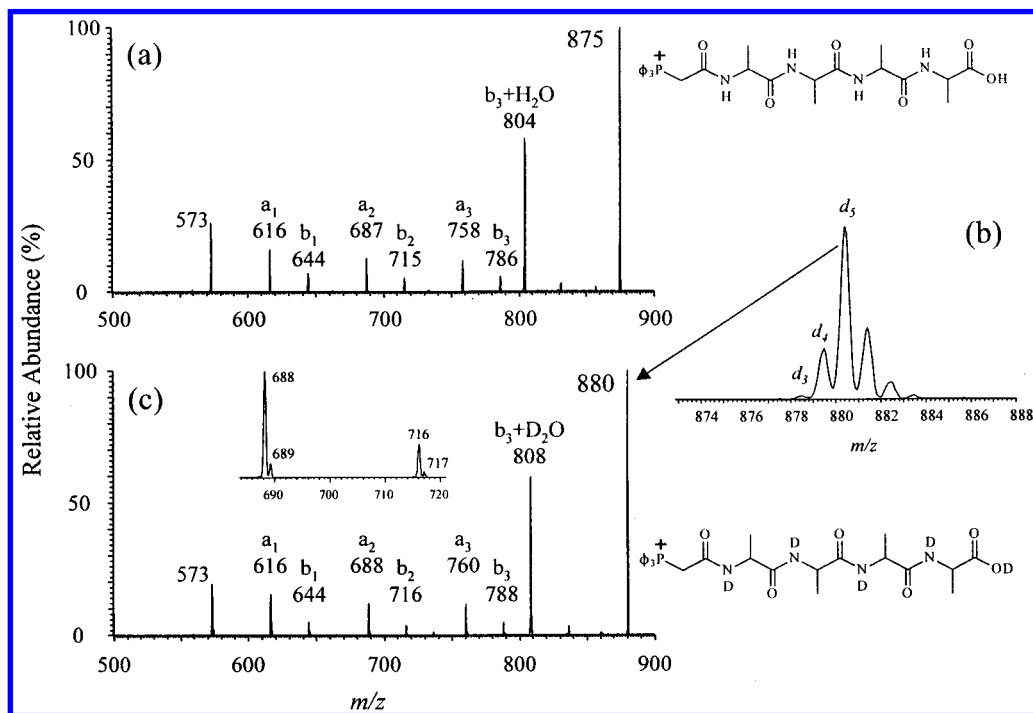


Figure 5. (a) ESI/CID spectra obtained in the ion trap instrument for singly charged ions of $\phi_3\text{P}^+\text{CH}_2\text{C}(=\text{O})\text{-AAAA}$, (b) molecular ion region of an ESI mass spectrum after H/D exchange for $\phi_3\text{P}^+\text{CH}_2\text{C}(=\text{O})\text{-AAAA}$ in deuterated solvent, and (c) ESI/CID spectra of $\phi_3\text{P}^+\text{CH}_2\text{C}(=\text{O})\text{-AAAA-d}_5$. The inset in part c shows the expanded region of the b_2/a_2 ions. The minor peaks such as m/z 689 and 717 shown in the inset are likely due to ^{13}C -contamination in parent ion selection (^{13}C -isotope peak of the peak labeled as d_4 in (b)). The CID spectra were acquired at $\sim 28\%$ "relative collision energy".

The structure of b ions formed at other amino acid residues in the presence of an ionizing proton ("generic" b ions) is commonly accepted to be a protonated oxazolone.^{28–31,53–55} In the case where charge is retained somewhere other than the cleaved site, a ketene-type structure $\text{C}(\text{R})=\text{C}=\text{O}$ has been suggested as a possible charge-remote b ion structure but the structure has not been proven.²¹ Deuterium labeling provides one means to address the question of the structure of the generic charge-remote b ions produced in the absence of an ionizing proton.

Figure 5 shows a comparison of the fragment ion masses for $\phi_3\text{P}^+\text{CH}_2\text{C}(=\text{O})\text{-AAAA}$, a peptide containing active hydrogens only at amide nitrogens and the C-terminus, and its H/D exchange product $\phi_3\text{P}^+\text{CH}_2\text{C}(=\text{O})\text{-AAAA-d}_5$. On the basis of the results of Figure 5a vs c, the numbers of deuteriums in the b ions of $\phi_3\text{P}^+\text{CH}_2\text{C}(=\text{O})\text{-AAAA-d}_5$ (part c) are 0, 1, and 2 for b_1 , b_2 , and b_3 ions, respectively. This indicates that a hydrogen/deuterium at the amide nitrogen migrates away from the N-terminal fragment in formation of the charge-remote b ions. The location of the transferred hydrogen, from the amide nitrogen and NOT from the α -carbon, shows that the most probable structure for a generic b ion is NOT a ketene structure but is instead a structure that involves cyclization or unsaturation at nitrogen. Scheme 4 (left) shows two possible structures for generic b ions produced from the N-terminal fixed-charge peptide derivative, i.e., possible b ion structures produced in the absence of an ionizing proton: a neutral oxazolone and a neutral aziridinone. (Note that, in the absence of an ionizing proton, the mechanism proposed for oxazolone formation in the presence of an ionizing proton (Scheme 1) cannot be operative.) Other possible structures include substituted small cyclic peptides. Previously, transfer of a hydrogen from the amide nitrogen of the N-terminal fragment has been shown in y ion

formation from protonated peptides.^{56,57} Wesdemiotis and co-workers investigated this transfer for the N-terminal neutral fragments by neutralization/reionization mass spectrometry (NRMS)^{53,58} and proposed an aziridinone structure when the N-terminal neutral fragment produced during the formation of a y ion is a single amino acid residue.⁵⁸

Although there are not enough data here to define the charge-remote b_n ion structure, any structure that is proposed must meet the following criteria. (i) The charge-remote b_n structure must explain the labeling results that are consistent with H(D) transfer away from the amide N in the formation of the b_n ions. (ii) The charge-remote b_n structure must allow for facile conversion of the b_n ions to the corresponding a_n ions. Both SID spectra (Figure 2a and SID spectrum of $\phi_3\text{P}^+\text{CH}_2\text{C}(=\text{O})\text{-AAAA}$ available in Supporting Information) and high-energy CID spectra reported in the literature³² for derivatized peptides, with the only charge provided by the phosphonium group at the amino terminus, contain dominant a_n ion series rather than b_n ion series (the exception being dominant b ions only at Asp–Xxx positions; see Figure 2a). The three-membered aziridinone structure, for example, might be more easily converted to a_n ions than would the

(53) Nold, M. J.; Wesdemiotis, C.; Yalcin, T.; Harrison, A. G. *Int. J. Mass Spectrom. Ion Processes* **1997**, *164*, 137–153.

(54) Vaisar, T.; Urban, J. *J. Mass Spectrom.* **1998**, *33*, 505–524.

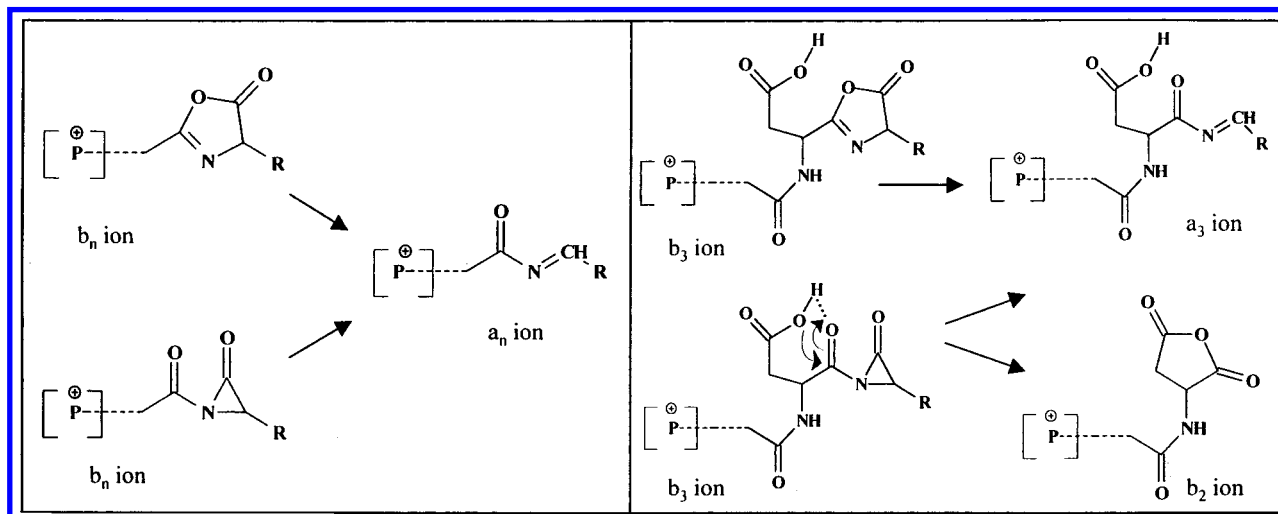
(55) The b ion produced by His–Xxx cleavage, in the presence of an ionizing proton, has a unique structure (not protonated oxazolone): Tsapralis, G.; Wysocki, V. H.; Zhong, W.; Nair, H.; Futrell, J., submitted for publication.

(56) Mueller, D. R.; Eckersley, M.; Richter, W. J. *Org. Mass Spectrom.* **1988**, *217*–222.

(57) Kenny, P. T. M.; Nomoto, K.; Orlando, R. *Rapid Commun. Mass Spectrom.* **1992**, *6*, 95–97.

(58) Cordero, M. M.; Houser, J. J.; Wesdemiotis, C. *Anal. Chem.* **1993**, *65*, 1594–1601.

Scheme 4



oxazolone, because of ring strain in the three-membered ring. (iii) The proposed charge-remote b_n ion structure must account for the difference in fragmentation of the b_4 and b_3 ions of $\phi_3\text{P}^+\text{CH}_2\text{C}(=\text{O})\text{-LDIFSDF}$ (Figure 4c). Note that the MS/MS/MS spectra of these two different b ions show that b_4 does not readily produce b_3 (Figure 4c inset) while b_3 readily produces b_2 (Figure 4c), suggesting the involvement of the Asp in the formation of b_2 . As an example, Scheme 4 (right) illustrates that the formation of b_2 from b_3 (by attack of the Asp side chain on the backbone) can be envisioned in a much more straightforward manner for the aziridinone than for the oxazolone. In summary, the labeling results show that hydrogen is lost from the amide nitrogen in the formation of charge-remote b ions, the labeling results thus suggest a charge-remote b ion with unsaturation or cyclization at the amide nitrogen, the charge-remote b_n ions produce a_n ions readily, and the charge-remote b_n ions give facile production of b_2 from b_3 in the fragmentation of $\phi_3\text{P}^+\text{CH}_2\text{C}(=\text{O})\text{-LDIFSDF}$. Additional studies are in progress to better define the structure of the charge remote b_n ions.

Formation of $b_{N-1} + \text{H}_2\text{O}$ Ions. The dominant fragment ions in Figure 5a and c correspond to a truncated peptide $b_{N-1} + \text{H}_2\text{O}$ ion (where N refers to the total number of amino acids in the peptide). The $b_{N-1} + \text{H}_2\text{O}$ ions were also produced in the dissociation spectra of $\phi_3\text{P}^+\text{CH}_2\text{C}(=\text{O})\text{-LDIFSDF}$, $\phi_3\text{P}^+\text{CH}_2\text{C}(=\text{O})\text{-LDIFSDFR}$, and $[\phi_3\text{P}^+\text{CH}_2\text{C}(=\text{O})\text{-LDIFSDFR} + \text{H}]^{2+}$. Gaskell and co-workers⁵⁹ suggested that these ions form via a seven-membered-ring H-bonded intermediate and five-membered-ring nucleophilic attack, similar to that suggested in Scheme 3 for cleavage at Asp–Xxx, followed by loss of NH-CH(R)CO . For $\phi_3\text{P}^+\text{CH}_2\text{C}(=\text{O})\text{-AAAA}$, this peak disappears when the methyl ester is fragmented. The $b_{N-1} + \text{H}_2\text{O}$ ions involve the carboxylic acid group of the carboxyl terminus and a fragmentation mechanism related to that proposed for Asp–Xxx cleavage. It is logical that this pathway can be favored under conditions similar to those that favor Asp–Xxx cleavage; i.e., when the charge is tightly bound elsewhere in the molecule, the acidic side chain or carboxy terminus causes selective dissociation. The $b_{N-1} + \text{H}_2\text{O}$ ion is

more dominant in the spectrum if no acidic residues are present (see Figure 5) or if Arg is present at the carboxy terminus (Figure in Supporting Information).

Competitive Nonselective Cleavage Promoted by a “Mobile” Proton. With a proton added to the peptide derivative $\phi_3\text{P}^+\text{CH}_2\text{C}(=\text{O})\text{-LDIFSDF}$, nonselective cleavages occur across the whole peptide backbone (Figures 1b and 2b). Previously, a general model for the fragmentation of protonated peptides, based on the “mobile proton”^{41,60} or equivalently, the “heterogeneously distributed proton”^{29,61,62} has evolved. The “mobile proton” model states that, in the absence of a strongly basic residue (e.g., Arg), the cleavages of various peptide bonds in protonated peptides occur following a migration of a mobile proton to the carbonyl oxygen and/or amide nitrogen of the backbone.^{41,60} In other words, the low-energy pathways that form b_n or y_n ions are promoted by charge-directed cleavage of peptide bonds initiated by a mobile available proton. For example, a proton located at the oxygen of an amide moiety promotes the nucleophilic attack by the adjacent backbone carbonyl oxygen on the carbonyl carbon of the protonated group (see Scheme 1) and, thus, promotes the formation of an oxazolone-structure b_n ion.^{28,29} The relative energetics of fragmentation for the Asp-containing fixed-charge peptide derivatives were investigated by SID. The ESI/SID fragmentation efficiency curves^{41,60} are provided in Figure 6. Approximately 75-eV collision energy is required to achieve 50% fragmentation for the $\phi_3\text{P}^+\text{CH}_2\text{C}(=\text{O})\text{-LDIFSDF}$ singly charged ions, whereas, for the doubly charged $[\text{M} + \text{H}]^{2+}$ ions with the addition of an extra proton to $\phi_3\text{P}^+\text{CH}_2\text{C}(=\text{O})\text{-LDIFSDF}$, the required collision energy for 50% fragmentation is dramatically lowered to ~ 20 eV (Figure 6). In Figure 6, the fragmentation efficiency (dashed line) for the doubly charged $[\text{M} + \text{H}]^{2+}$ ions of $\phi_3\text{P}^+\text{CH}_2\text{C}(=\text{O})\text{-LDIFSDFR}$ is decreased (i.e., the curve is shifted to higher collision energies) relative to that of the $[\text{M} + \text{H}]^{2+}$ ions of $\phi_3\text{P}^+\text{CH}_2\text{C}(=\text{O})\text{-LDIFSDF}$. The fact that the two curves for doubly charged ions shift to

(60) Jones, J. L.; Dongré, A. R.; Somogyi, Á.; Wysocki, V. H. *J. Am. Chem. Soc.* **1994**, *116*, 8368–8369.

(61) Burlet, O.; Orkiszewski, R. S.; Ballard, K. D.; Gaskell, S. J. *Rapid Commun. Mass Spectrom.* **1992**, *6*, 658–662.

(62) Cox, K. A.; Gaskell, S. J.; Morris, M.; Whiting, A. *J. Am. Soc. Mass Spectrom.* **1996**, *7*, 522–531.

(59) Thorne, G. C.; Ballard, K. D.; Gaskell, S. J. *J. Am. Soc. Mass Spectrom.* **1990**, *1*, 249–257.

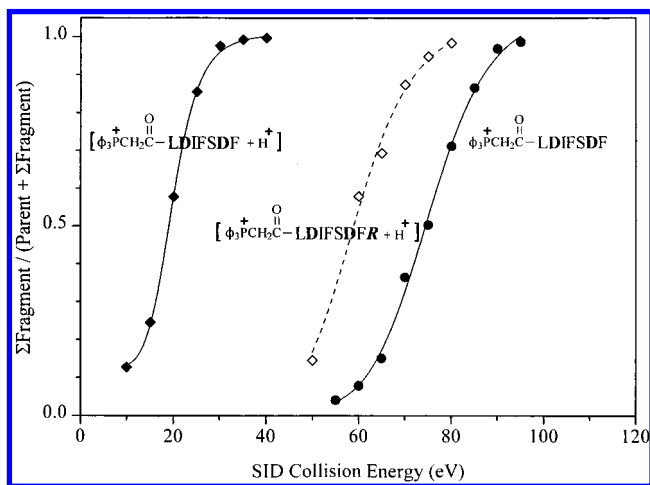


Figure 6. ESI/SID fragmentation efficiency curves for M^+ ions of $\phi_3P^+CH_2C(=O)-LDIFSDF$, $[M + H]^{2+}$ ions of $\phi_3P^+CH_2C(=O)-LDIFSDF$, and $[M + H]^{2+}$ ions of $\phi_3P^+CH_2C(=O)-LDIFSDFR$. The collision target surface used in SID is a SAM surface of $CF_3(CF_2)_9-CH_2CH_2S-Au$.

different positions suggests that the shift in the ESI/SID fragmentation efficiency curves of the doubly charged ions versus the singly charged ion is *not* simply a charge effect (e.g., Coulombic repulsion). It has been previously reported in the literature that a multiply protonated ion at a higher charge state does *not necessarily* fragment more easily than that at a lower charge state.^{15,63} Because the guanidino group of the arginine residue is highly basic, the added proton in the $[M + H]^{2+}$ ions of $\phi_3P^+CH_2C(=O)-LDIFSDFR$ is most likely retained by the Arg side chain. For the derivative $\phi_3P^+CH_2C(=O)-LDIFSDF$ without an Arg residue, the *available mobile proton*, but *not* the facile fragmentation simply due to two charges, makes the fragmentation much easier for the $[M + H]^{2+}$ ions relative to the M^+ ions (see the relative positions of the two solid curves in Figure 6). This suggests that charge-directed fragmentation channels due to an available mobile proton (e.g., acid-catalyzed formation^{28,29,54} of oxazolone-like b_n ions or the corresponding y -type ions) are favored kinetically (five-ring attack) over those catalyzed by Asp residues (seven-ring intermediate leading to five-ring attack) as described in Scheme 3. As a result, selective cleavages at Asp-Xxx are no longer dominant when a mobile proton is available.

CONCLUSIONS

In conclusion, the present results unequivocally demonstrate that, in the absence of an available mobile proton, selective cleavages at a peptide bond immediately C-terminal to an Asp residue (Asp-Xxx) dominate the MS/MS spectra of charged

peptides. Their occurrence in MS/MS measurements of Asp-containing peptides is proposed to be promoted by a seven-membered-ring H-bonded structure involving the acidic hydrogen of the Asp side chain. The resulting product b_n ion is accordingly a succinic anhydride five-membered cyclic structure as supported by MS^3 experimental results. In the presence of an available mobile proton, onset energies for dissociation are lowered significantly and low-energy dissociation pathways that presumably involve proton-catalyzed formation of oxazolone-type structures are favored over the cleavages promoted by the cyclic H-bonding involving the Asp side chain. This leads to nonselective fragmentation patterns, as well as improved fragmentation efficiencies. The b_n ions formed at Asp in the absence or presence of a mobile proton and a fixed charge have an anhydride structure that further fragments to form d_n and c_{n-1} ions. In contrast, the "generic" b_n ions produced by a charge-remote mechanism from singly charged fixed-charge peptide derivatives are suggested to be cyclic structures that readily fragment to produce a_n ions.

The results presented in this and related papers will help strengthen the analytical utility of MS-based sequencing protocols by providing improved and additional predictive rules of peptide dissociation for computer-aided interpretation of MS/MS spectra. The data described here and in our earlier work show that enhanced/selective cleavage occurs at Asp-Xxx sites when the ionizing charge is sequestered at arginine. When protons in excess of the number of Arg are present, enhanced/selective cleavages at Asp-Xxx are not expected.

ACKNOWLEDGMENT

This work was financially supported by a grant from the National Institutes of Health (GM RO151387 to V.H.W.) and a postdoctoral fellowship from the Fonds pour la Formation de Chercheurs et l'Aide à la Recherche (to G.T.). We thank Dr. Arpad Somogyi for his help and use of the LCQ instrument at the Mass Spectrometry Facility in the Chemistry Department at the University of Arizona.

SUPPORTING INFORMATION AVAILABLE

Supporting Information is available for the spectra not shown: ESI/CID of $\phi_3P^+CH_2C(O)-LDIFSDF$ at relatively higher collision energy, ESI/CID of $\phi_3P^+CH_2C(O)-LDIFSDFR$, MS^3 of the d_2 ion of $\phi_3P^+CH_2C(O)-LDIFSDF$, MS^3 of the b_6 ion of $\phi_3P^+CH_2C(O)-LDIFSDF$, ESI/CID of $\phi_3P^+CH_2C(O)-LDIFSDF-d_{11}$, MS^3 of the b_6 ion of $[\phi_3P^+CH_2C(O)-LDIFSDF + H]^{2+}$, MS^3 of the b_6 ion of $[LDIFSDF + H]^+$, MS^3 of the b_4 ion of $[LDIFSDF + H]^+$, and SID of $\phi_3P^+CH_2C(O)-AAAA$. This material is available free of charge via the Internet at <http://pubs.acs.org>.

Received for review May 15, 2000. Accepted September 27, 2000.

AC000555C

(63) de Maaijer-Gielbert, J.; Gu, C.; Somogyi, A.; Wysocki, V. H.; Kistemaker, P. G.; Weeding, T. L. *J. Am. Soc. Mass Spectrom.* **1999**, *10*, 414–422.